doi:10.1038/nature07726

LETTERS

Chromatin remodelling factor *Mll1* is essential for neurogenesis from postnatal neural stem cells

Daniel A. Lim[1,2,3]*, Yin-Cheng Huang[1,2]*†, Tomek Swigut[4], Anika L. Mirick[5], Jose Manuel Garcia-Verdugo[6,7], Joanna Wysocka[4], Patricia Ernst[5] & Arturo Alvarez-Buylla[1,2]

Epigenetic mechanisms that maintain neurogenesis throughout adult life remain poorly understood[1]. Trithorax group (trxG) and Polycomb group (PcG) gene products are part of an evolutionarily conserved chromatin remodelling system that activate or silence gene expression, respectively[2]. Although PcG member *Bmi1* has been shown to be required for postnatal neural stem cell self-renewal[3,4], the role of trxG genes remains unknown. Here we show that the trxG member *Mll1* (*mixed-lineage leukaemia 1*) is required for neurogenesis in the mouse postnatal brain. *Mll1*-deficient subventricular zone neural stem cells survive, proliferate and efficiently differentiate into glial lineages; however, neuronal differentiation is severely impaired. In *Mll1*-deficient cells, early proneural *Mash1* (also known as Ascl1) and gliogenic *Olig2* expression are preserved, but *Dlx2*, a key downstream regulator of subventricular zone neurogenesis, is not expressed. Overexpression of *Dlx2* can rescue neurogenesis in *Mll1*-deficient cells. Chromatin immunoprecipitation demonstrates that *Dlx2* is a direct target of MLL in subventricular zone cells. In differentiating wild-type subventricular zone cells, *Mash1*, *Olig2* and *Dlx2* loci have high levels of histone 3 trimethylated at lysine 4 (H3K4me3), consistent with their transcription. In contrast, in *Mll1*-deficient subventricular zone cells, chromatin at *Dlx2* is bivalently marked by both H3K4me3 and histone 3 trimethylated at lysine 27 (H3K27me3), and the *Dlx2* gene fails to properly activate. These data support a model in which *Mll1* is required to resolve key silenced bivalent loci in postnatal neural precursors to the actively transcribed state for the induction of neurogenesis, but not for gliogenesis.

Neural stem cells (NSCs) and neurogenesis persist throughout life in the subventricular zone (SVZ) and dentate gyrus of the hippocampus. The *Mll1* histone methyltransferase is expressed in adult SVZ cells[5] as well as embryonic SVZ and ventricular zone (Supplementary Fig. 1). In development, *Mll1* regulates the epigenetic maintenance of homeotic gene expression patterns[2]. Human *MLL* is a proto-oncogene, with chromosomal translocations resulting in MLL fusion proteins that produce human leukaemias with mixed lineage identity[6]. Mouse *Mll1* is required for embryonic haematopoiesis, and most *Mll1*-null mice die between embryonic day (E)10.5 and E12 (ref. 7). We therefore used a conditional knockout 'floxed' allele of *Mll1* (*Mll1*$^{F/F}$)[8].

To delete *Mll1* from a subset of NSCs, we used the transgenic mouse *hGFAP-Cre*[9], which exhibits excision of floxed alleles in precursors of the hippocampal dentate gyrus, cerebellar granular cells, and SVZ NSCs at E13.5 (ref. 10). *hGFAP-Cre;Mll1*$^{F/F}$ mice were born at the expected Mendelian ratios and were indistinguishable from their wild-type and *hGFAP-Cre;Mll1*$^{F/+}$ littermates (hereafter referred to as controls). However, by postnatal day (P)15, *hGFAP-Cre;Mll1*$^{F/F}$ mice developed progressive growth retardation and ataxia, and the mice usually died between P25 and P30. We therefore initially analysed *hGFAP-Cre;Mll1*$^{F/F}$ mice and controls at P23–P25.

All brain regions that undergo considerable postnatal neurogenesis—including the cerebellar granule cell layer, hippocampal dentate gyrus (Supplementary Fig. 2) and the olfactory bulb (Fig. 1b)—showed a marked reduction in the size and the number of neurons in *hGFAP-Cre;Mll1*$^{F/F}$ mice. This suggested a common requirement for *Mll1* in neurogenesis. To investigate the role of *Mll1* in a NSC population, we focused on the SVZ-olfactory-bulb system. Throughout life, NSCs in the SVZ generate large numbers of neuroblasts that migrate to the olfactory bulb[11–13] where they differentiate into interneurons (Fig. 1a, schematic). To evaluate the rate of SVZ neurogenesis, we injected animals with the cell-cycle marker 5-bromo-2-deoxyuridine (BrdU) 1 h before being culled and then co-immunostained sections for BrdU and the neuroblast marker doublecortin (DCX). *hGFAP-Cre;Mll1*$^{F/F}$ mice had 3–4-fold fewer BrdU$^+$ DCX$^+$ SVZ cells than the controls (Fig. 1c, d). Despite this decreased rate of BrdU incorporation, *hGFAP-Cre;Mll1*$^{F/F}$ mice had an expanded SVZ (Fig. 1c, right, yellow doubleheaded arrow) containing DCX$^+$ cells; this accumulation developed after P7 (Supplementary Fig. 3) and could be explained if *Mll1*-deficient progenitor cells have impaired and/or abnormal migration, resulting in cell accumulation. Although *Mll1*-deficient progenitors retained expression of neuroblast markers such as DCX and Tuj1 (Supplementary Fig. 3), they also possessed ultrastructural characteristics of intermediate, transit-amplifying cells (Supplementary Fig. 5k, l). Indeed, neuroblast chain migration in *hGFAP-Cre;Mll1*$^{F/F}$ mice and from SVZ explants[14] was severely disorganized, resulting in a 40% reduction in the migration distance *in vitro* (Supplementary Fig. 4). Thus, postnatal neuronal addition in the olfactory bulb was abrogated by a decreased rate of neurogenesis as well as by impaired neuroblast migration.

In addition to producing neurons, SVZ NSCs generate astrocytes and oligodendrocytes[15–17]. Glial development in *hGFAP-Cre;Mll1*$^{F/F}$ mice was not impaired. In fact, expression of the astrocyte marker GFAP was increased in the SVZ of *hGFAP-Cre;Mll1*$^{F/F}$ mice (Fig. 2a) as well as in other brain regions (Supplementary Fig. 5e–h). The SVZ ependymal layer develops postnatally[18], and these cells formed normally in *hGFAP-Cre;Mll1*$^{F/F}$ mice (Fig. 2b and Supplementary Fig. 5i, j). OLIG2 is expressed in developing and mature oligodendrocytes[19,20], and OLIG2 expression in white matter was similar in

[1]Department of Neurological Surgery, [2]Institute for Regeneration Medicine, and [3]Veteran's Affairs Medical Center, University of California, San Francisco, 505 Parnassus Street M779, San Francisco, California 94143, USA. [4]Department of Chemical and Systems Biology, Department of Developmental Biology Stanford University School of Medicine, Stanford, California 94305, USA. [5]Department of Genetics, Dartmouth Medical School, Hanover, New Hampshire 03755, USA. [6]Laboratorio de Neurobiologia Comparada, Instituto Cavanilles, Universidad de Valencia, Valencia 46012, Spain. [7]Laboratorio de Morfologia Celular, Centro de Investigación Príncipe Felipe, CIBERNED, Valencia 46012, Spain. †Present address: Department of Neurosurgery, Graduate Institute of Clinical Medical Science, ChangGung Univerisity, Kwei-Shan, Tao-yuan, Taiwan.
*These authors contributed equally to this work.

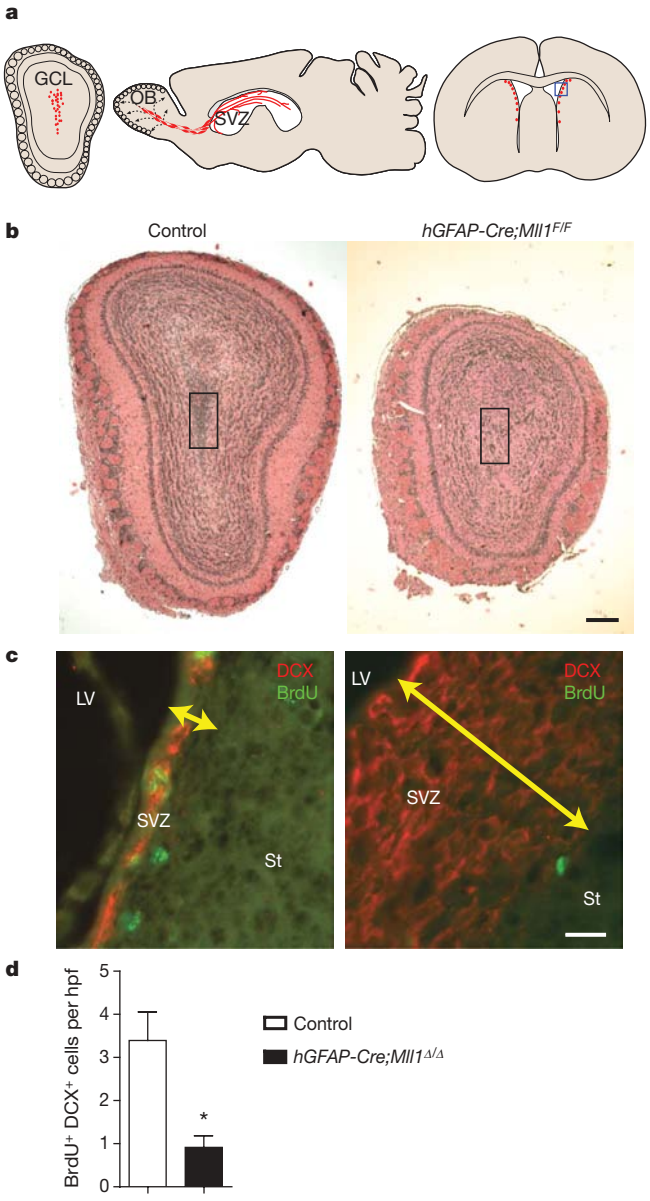

Figure 1 | *Mll1* is required for normal SVZ-olfactory bulb neurogenesis. **a**, Schematics of SVZ-olfactory-bulb neurogenesis. Left, coronal section of the olfactory bulb (OB) indicating the region where newly born neuroblasts (red dots) initially arrive from the SVZ. GCL, granule cell layer. Middle, sagittal section showing paths of neuroblast migration from the SVZ to the olfactory bulb. Right, coronal section indicating the germinal SVZ (red dots); the blue box indicates regions shown in **c**. **b**, Haematoxylin and eosin (H&E)-stained coronal sections through the P25 olfactory bulb of control (left) and *hGFAP-Cre;Mll1*$^{F/F}$ (right) mice. The black box indicates the olfactory bulb core comprised of recently born neuroblasts. **c**, DCX (red) and BrdU (green) immunohistochemistry of the SVZ is shown. The size of the SVZ is indicated by a yellow doubleheaded arrow. LV, lateral ventricle; St, striatum. **d**, Quantification of BrdU$^+$ DCX$^+$ SVZ cells. hpf, high power field. Error bars, s.e.m.; three mice per group; *$P = 0.025$. Scale bars, 200 μm (**b**) and 20 μm (**c**).

hGFAP-Cre;Mll1$^{F/F}$ mice and controls (Fig. 2c, green). Furthermore, oligodendrocyte myelination of major axon tracts in *hGFAP-Cre;Mll1*$^{F/F}$ mice appeared normal as assessed by FluoroMyelin staining (Supplementary Fig. 5a–d) and myelin basic protein (MBP) immunohistochemistry (Fig. 2c, red). However, it was possible that local, non-SVZ glial progenitors had compensated for a defective SVZ stem cell population.

Therefore, to specifically examine the developmental potential of SVZ stem cells, we used SVZ monolayer NSC cultures[21]. MLL1 was

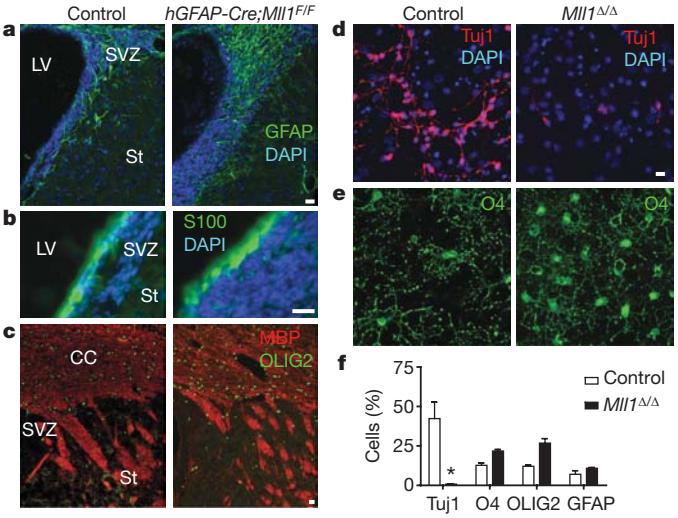

Figure 2 | *Mll1*-deletion impairs postnatal SVZ-olfactory-bulb neurogenesis but not gliogenesis. **a**, Immunohistochemistry for the astrocyte marker GFAP (green) in P25 coronal brain sections of control (left) and *hGFAP-Cre;Mll1*$^{F/F}$ (right) mice. Nuclei are counterstained with 4,6-diamidino-2-phenylindole (DAPI; blue). **b**, Immunohistochemistry for the S100$^+$ (green) ependymal cells. **c**, Immunohistochemistry for markers of oligodendrocytes, OLIG2 (green) and MBP (red). CC, corpus callosum. **d**, SVZ cultures after 4 days of differentiation from control (left) and *Mll1*$^{Δ/Δ}$ (right) mice immunostained for the neuronal marker Tuj1 (red). **e**, O4$^+$ (green) oligodendrocytes in the same fields of view as those in **d**. **f**, Quantification of cell differentiation. Error bars, s.e.m. of triplicate cultures; *$P = 0.016$. Scale bars, 20 μm.

expressed in control SVZ cultures, whereas cultures from *hGFAP-Cre;Mll1*$^{F/F}$ mice were 95–96% MLL1-deleted (Supplementary Fig. 6a–e). *Mll1*$^{Δ/Δ}$ and control SVZ cultures had similar proliferation rates (27.5% ± 0.7% BrdU$^+$ cells in *Mll1*$^{Δ/Δ}$ cultures versus 26.7% ± 2.4% in controls; mean ± s.e.m.). In differentiation conditions, *Mll1*$^{Δ/Δ}$ cultures produced >20-fold fewer Tuj1$^+$ cells compared to controls (Fig. 2d, f). *Mll1*$^{Δ/Δ}$ cultures had comparable numbers of pycnotic cells under both proliferative (79% of control, 31% s.d.) and differentiation (68% of control, 15% s.d.) conditions, suggesting that *Mll1* was not required for SVZ cell survival. Similar to our observations *in vivo*, *Mll1*$^{Δ/Δ}$ cultures efficiently produced GFAP$^+$ astrocytes and O4$^+$ and OLIG2$^+$ oligodendrocytes (Fig. 2e, f and Supplementary Fig. 6i, j). Thus, *Mll1*$^{Δ/Δ}$ SVZ NSC cultures had a similar proliferation rate and comparable cell death rate, but they produced fewer neuronal cells while remaining gliogenic.

Because *Mll1* was deleted in radial glial precursors at E13.5, it was possible that many transcriptional changes had 'accumulated' before the genesis of SVZ NSCs. Therefore, we next studied the effect of *Mll1* deletion after postnatal SVZ NSC genesis. To accomplish this, we derived SVZ NSC cultures from P6–P7 *Mll1*$^{F/F}$ or *Mll1*$^{+/+}$ mice that also carried the *ZEG* reporter transgene; *ZEG* expresses green fluorescent protein (GFP) in cells that have undergone Cre-mediated recombination[22]. Cultures were then infected with an adenovirus expressing Cre, and 48–72 h later GFP$^+$ cells were isolated by fluorescent activated cell sorting (FACS) (Supplementary Fig. 7a). Ninety-five to ninety-eight per cent of GFP$^+$ *Mll1*$^{F/F}$;*ZEG* cells (hereafter referred to as *ZEG;Mll1*$^{Δ/Δ}$ cells) did not express MLL1; conversely, 100% of GFP$^+$ *Mll1*$^{+/+}$;*ZEG* cells (hereafter referred to as ZEG; control cells) expressed MLL1 protein (Supplementary Fig. 7b–e). There was no significant difference in cell death between proliferating *ZEG;Mll1*$^{Δ/Δ}$ and ZEG;control stem cell cultures as assessed by propidium iodide and annexin A5 staining (Supplementary Fig. 7f). After FACS isolation, *ZEG;Mll1*$^{Δ/Δ}$ and ZEG;control cells also had similar BrdU incorporation rates (Supplementary Fig. 7g). Under differentiation conditions, *ZEG;Mll1*$^{Δ/Δ}$ SVZ cells produced three-fold fewer Tuj1$^+$ cells than ZEG;control cells (Fig. 3a–c).

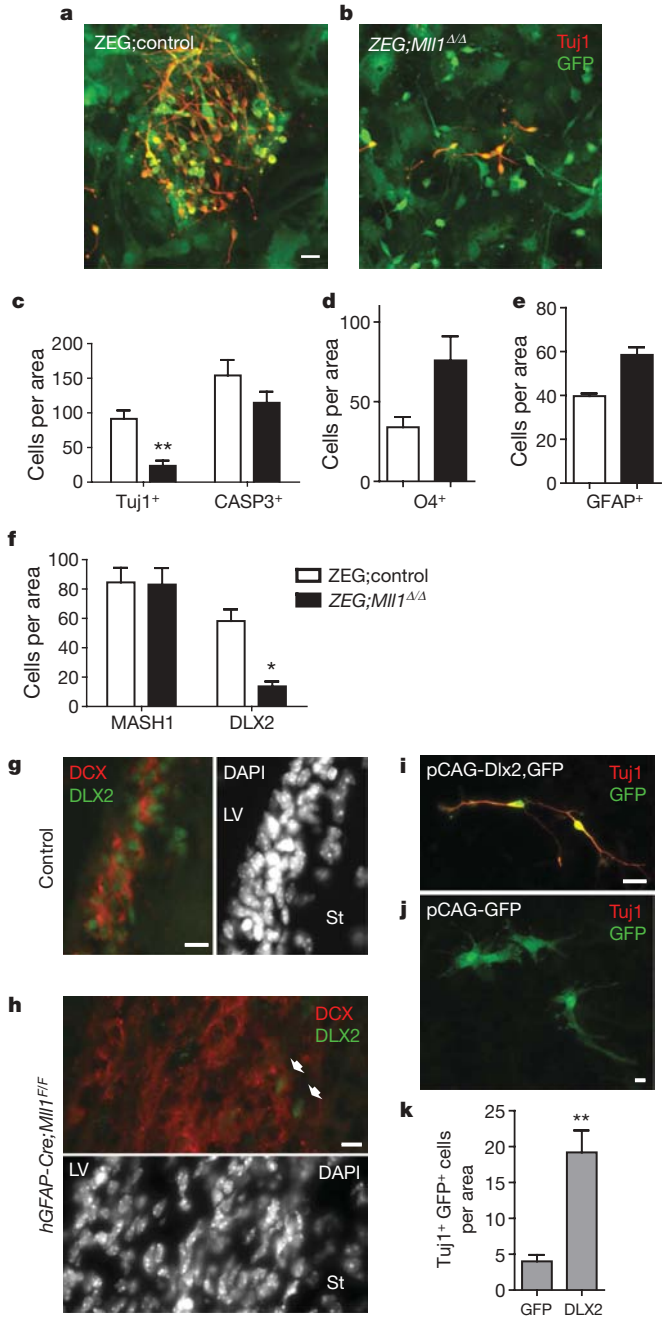

Figure 3 | *Mll1*-dependent DLX2 expression is required for postnatal SVZ neurogenesis. **a**, Immunocytochemistry for Tuj1$^+$ (red) neuroblasts in FACS-isolated GFP$^+$ ZEG;control SVZ cells after differentiation. **b**, *ZEG;Mll1*$^{\Delta/\Delta}$ cultures stained for Tuj1. **c**, Quantification of Tuj1$^+$ neuronal differentiation and activated caspase 3$^+$ cells after 4 days of differentiation. $^{**}P = 0.002$. **d**, **e**, Quantification of glial differentiation. The number of O4$^+$ oligodendrocytes (**d**) and GFAP$^+$ astrocytes (**e**) was counted after 4–5 days of differentiation. **f**, Quantification of MASH1$^+$ and DLX2$^+$ cells after 2 days of differentiation. $^{*}P = 0.02$. **g**, **h**, Immunohistochemistry for DLX2 (green) and DCX (red) in SVZ coronal brain sections of control (**g**) and *hGFAP-Cre;Mll1*$^{F/F}$ mice (**h**). **i**–**k**, Enforced *Dlx2* expression can rescue neurogenesis in *Mll1*$^{\Delta/\Delta}$ SVZ cultures. Immunocytochemistry for Tuj1 (red) and GFP (green) after transfection of both pCAG-Dlx2 and pCAG-GFP plasmids (**i**) and pCAG-GFP plasmid alone (**j**). **k**, Quantification of neuronal lineage rescue by *Dlx2* transfection. $^{**}P = 0.004$; error bars, s.e.m.; 3–6 replicates per group. Scale bars, 10 μm (**g**, **h**) and 20 μm (**a**, **b**, **i**, **j**).

Differentiating *ZEG;Mll1*$^{\Delta/\Delta}$ cells had a trend towards fewer activated caspase 3$^+$ cells (Fig. 3c), indicating that cell death did not account for the decreased neurogenesis. Furthermore, *ZEG;Mll1*$^{\Delta/\Delta}$ cells produced glial populations efficiently; in fact, there was approximately twofold more O4$^+$ oligodendrocytes and 50% more GFAP$^+$ astrocytes (Fig. 3d, e and Supplementary Fig. 7h, i) in *ZEG;Mll1*$^{\Delta/\Delta}$ SVZ cultures. Thus, *Mll1* was required after the genesis of SVZ stem cells specifically for the neuronal lineage.

Because *Mll1* is important for the epigenetic regulation of specific gene expression, we next examined the expression of genes important for SVZ neurogenesis. NSC markers SOX2 (ref. 23) and Nestin were present in 100% of cells in both *ZEG;Mll1*$^{\Delta/\Delta}$ and ZEG;control cells under proliferation conditions (Supplementary Fig. 7j, k). During early differentiation, MASH1 expression, a bHLH factor important for SVZ neurogenesis and oligodendrogliogenesis[24], was also not altered in *ZEG;Mll1*$^{\Delta/\Delta}$ cultures (Fig. 3f and Supplementary Fig. 8a, b). However, DLX2, a homeodomain-containing transcription factor important for olfactory bulb interneuron development and migration in the embryo[25], was decreased ~fourfold in *ZEG;Mll1*$^{\Delta/\Delta}$ cultures (Fig. 3f and Supplementary Fig. 8c, d). *In vivo* immunostaining showed a similar impairment of DLX2 expression in the SVZ of *hGFAP-Cre;Mll1*$^{F/F}$ mice (Fig. 3g, h). Normally, *Dlx2* is expressed in transit-amplifying cells and is then maintained in migratory neuroblasts. *hGFAP-Cre;Mll1*$^{F/F}$ mice still had DLX2 in a few cells at the base of the mass of DCX$^+$ cells, however, most these cells did not express this transcription factor.

To demonstrate that *Dlx2* is a key developmental regulator for *Mll1*-dependent neurogenesis, we co-transfected *Dlx2* and GFP expression plasmids into *Mll1*$^{\Delta/\Delta}$ SVZ cultures and induced differentiation. Transfection of the GFP plasmid alone was performed as a control. Concordance of GFP and DLX2 expression in co-transfected cultures was ~85% (Supplementary Fig. 9a, b). *Mll1*$^{\Delta/\Delta}$ SVZ cells co-transfected with *Dlx2* and GFP had a fourfold increase in the number of Tuj1$^+$ GFP$^+$ cells (Fig. 3i, quantification in panel k) after 4 days of differentiation as compared to the GFP-transfected controls (Fig. 3j).

To determine whether *Dlx2* is a direct target of MLL1, we performed chromatin immunoprecipitation (ChIP) from differentiating SVZ NSC cultures with anti-MLL1 antibodies. We found that MLL1 specifically bound to the *Dlx2* promoter region and the region immediately downstream from the transcriptional start site, but not to the chromatin 1 kb upstream (Fig. 4a).

Methylation of histone lysine residues is a critical determinant of active and silent gene expression states. H3K4me3 correlates strongly with active transcription whereas H3K27me3 is associated with gene silencing. Chromatin regions containing high levels of both H3K4me3 and H3K27me3 have been termed 'bivalent domains' and are silenced but thought to be 'poised' for activation[26]. MLL contains a catalytic SET domain that can methylate histone H3 at K4 (ref. 27). MLL family members can also recruit H3K27-specific histone demethylases[28,29]. Thus MLL proteins possess two non-mutually exclusive mechanisms for promoting transitions between transcriptionally restrictive and permissive chromatin states. We therefore investigated H3 methylation patterns at the promoter regions of *Dlx2*, *Mash1* and *Olig2*. In differentiating SVZ cells, *Dlx2* expression was *Mll1*-dependent whereas *Mash1* and *Olig2* expression were not (Fig. 4b). ChIP analysis of wild-type cells demonstrated that there were high levels of H3K4me3 and low levels of H3K27me3 at all three loci, coherent with their transcriptionally active state (Fig. 4c, d, yellow bars). Surprisingly, loss of MLL1 did not affect H3K4me3 at any of the analysed loci, suggesting that other H3K4 methyltransferases are important for maintenance of H3K4me3 at the *Dlx2* locus. In *Mll1*$^{\Delta/\Delta}$ cells, H3K27me3 levels were strongly increased at *Dlx2*, but not at *Mash1* or *Olig2* loci (Fig. 4d, brown bars). Moreover, in the absence of MLL1, we observed H3K27me3 spreading 1 kb upstream of the transcriptional start site (Fig. 4d), consistent with previous descriptions of bivalent loci[30]. Thus, in the absence of MLL1, the *Dlx2* locus is bivalent in differentiating SVZ NSCs.

Bivalent domains mark developmentally important loci in pluripotent and multipotent cells[26]. Upon differentiation into lineage-specific precursors, many bivalent domains are resolved into H3K4me3 or H3K27me3 monovalent domains, However, some loci

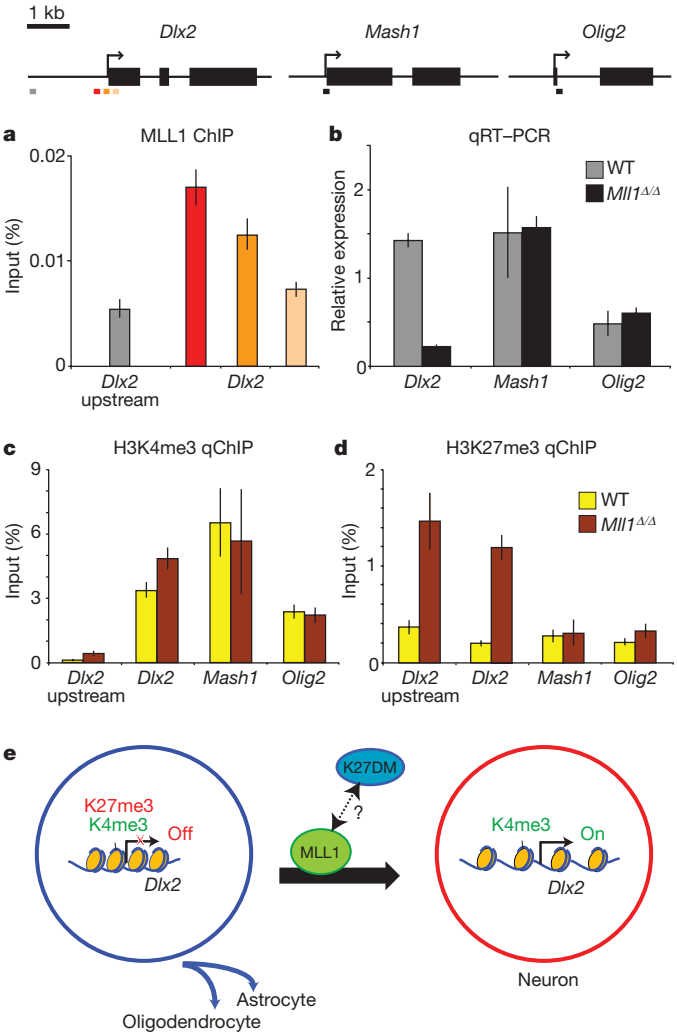

Figure 4 | *Dlx2* is trimethylated at both H3K4 and H3K27 in *Mll1*$^{\Delta/\Delta}$ cells. At the top is a schematic indicating the location of the primer sets used for qChIP. **a**, MLL1 qChIP of the *Dlx2* locus. **b**, qRT–PCR analysis of *Dlx2*, *Mash1* and *Olig2* in wild-type (grey bars) and *Mll1*$^{\Delta/\Delta}$ (black bars) cells during early differentiation. **c**, qChIP analysis of H3K4me3 levels at *Dlx2*, *Mash1* and *Olig2* loci. **d**, qChIP for H3K27me3 levels. **e**, Model of *Mll1* function in the specification of the neuronal lineage from NSCs. NSCs have bivalent chromatin domains at key neurogenic genes (for example, *Dlx2*). In this state, precursors can form astrocytes and oligodendrocytes (blue arrows). In order for neurogenesis to proceed (red arrow), MLL1 is required for the resolution of specific bivalent loci, possibly by recruiting H3K27-specific demethylases (K27DM). Error bars, s.d.; $n = 3$.

remain bivalent[30], possibly reflecting remaining gene expression plasticity. The presence of bivalent domains in tissue-specific stem cell populations suggests that there is a requirement for H3K27me3 demethylase activity at specific loci throughout development, and, in the case of SVZ neurogenesis, into adulthood. Our data are consistent with a model in which MLL1 function, perhaps mediated by H3K27me3 demethylase recruitment, is essential for bivalent domain resolution at *Dlx2* during neurogenesis (Fig. 4e). In the absence of MLL1, the *Dlx2* locus remains bivalent and therefore silenced. Deletion of *Mll1* in broader and/or earlier populations of NSCs in development may reveal a similar requirement of *Mll1* for embryonic neurogenesis.

Taken together, our results indicate that for lifelong neurogenesis, *Mll1* is required by neural precursors to make the epigenetic transition to the neuronal lineage by mediating chromatin modifications at specific loci. Future analysis of the direct targets of MLL and bivalent loci in NSCs at different stages of development may lead to an epigenetic description of NSC lineage potential and a transcriptional program instructive for neurogenesis.

METHODS SUMMARY

Mll1$^{F/F}$ mice were maintained and genotyped as described[8]. For immunocytochemistry, frozen sections were used. Tissue preparation for electron microscopy was performed with standard techniques[13]. For cell culture, mouse SVZ monolayer cultures were derived and grown essentially as previously described[21]. FACS was performed with a FACSAria cell sorter (BD Biosciences). Annexin A5 staining was quantified with a FACS Vantage flow cytometer (BD Biosciences). Transfection of SVZ cells was performed with Lipofectamine (Invitrogen). Paraformaldyhyde-fixed cultures were immunostained using standard protocols. For quantification of cell cultures, at least five non-overlapping high-power fields of view were analysed. SVZ cells *in vivo* were quantified from multiple non-overlapping confocal optical sections obtained with a Zeiss Axiovert 200M. Statistical analysis was performed using GraphPad Prism software; unpaired *t*-tests were used for the two-way comparisons. For quantitative PCR with reverse transcription (qRT–PCR), RNA was isolated with Trizol (Invitrogen), treated with DNase, and reverse transcribed using VILO Superscript (Invitrogen). qPCR was performed with the Roche LC480 using SybrGreen (Roche). Relative gene expression was normalized to six housekeeping genes. For quantitative ChIP (qChIP), chromatin was prepared from cells fixed with 1% formaldehyde and then sheered by sonication. Chromatin was incubated overnight with the indicated antibodies, and then collected by incubation with Protein A Dynabeads (Invitrogen). DNA eluted from the washed immune complexes was extracted, precipitated and then subjected to qPCR analysis with SybrGreen. Recovery of genomic DNA as a percentage input was calculated as the ratio of copy numbers in the precipitated immune complexes to the input control.

Full Methods and any associated references are available in the online version of the paper at www.nature.com/nature.

Received 23 July 2007; accepted 15 December 2008.
Published online 11 February 2009.

1. Hsieh, J. & Gage, F. H. Epigenetic control of neural stem cell fate. *Curr. Opin. Genet. Dev.* **14,** 461–469 (2004).
2. Schuettengruber, B., Chourrout, D., Vervoort, M., Leblanc, B. & Cavalli, G. Genome regulation by polycomb and trithorax proteins. *Cell* **128,** 735–745 (2007).
3. Molofsky, A. V. *et al.* Bmi-1 dependence distinguishes neural stem cell self-renewal from progenitor proliferation. *Nature* **425,** 962–967 (2003).
4. Fasano, C. A. *et al.* shRNA knockdown of *Bmi-1* reveals a critical role for p21-Rb pathway in NSC self-renewal during development. *Cell Stem Cell* **1,** 87–99 (2007).
5. Lim, D. A. *et al. In vivo* transcriptional profile analysis reveals RNA splicing and chromatin remodeling as prominent processes for adult neurogenesis. *Mol. Cell. Neurosci.* **31,** 131–148 (2006).
6. Daser, A. & Rabbitts, T. H. Extending the repertoire of the mixed-lineage leukemia gene *MLL* in leukemogenesis. *Genes Dev.* **18,** 965–974 (2004).
7. Yu, B. D., Hess, J. L., Horning, S. E., Brown, G. A. & Korsmeyer, S. J. Altered Hox expression and segmental identity in *Mll*-mutant mice. *Nature* **378,** 505–508 (1995).
8. Jude, C. D. *et al.* Unique and independent roles for MLL in adult hematopoietic stem cells and progenitors. *Cell Stem Cell* **1,** 324–337 (2007).
9. Zhuo, L. *et al.* hGFAP-cre transgenic mice for manipulation of glial and neuronal function *in vivo*. *Genesis* **31,** 85–94 (2001).
10. Han, Y. G. *et al.* Hedgehog signaling and primary cilia are required for the formation of adult neural stem cells. *Nature Neurosci.* **11,** 277–284 (2008).
11. Luskin, M. B. Restricted proliferation and migration of postnatally generated neurons derived from the forebrain subventricular zone. *Neuron* **11,** 173–189 (1993).
12. Lois, C. & Alvarez-Buylla, A. Long-distance neuronal migration in the adult mammalian brain. *Science* **264,** 1145–1148 (1994).
13. Doetsch, F., Caille, I., Lim, D. A., Garcia-Verdugo, J. M. & Alvarez-Buylla, A. Subventricular zone astrocytes are neural stem cells in the adult mammalian brain. *Cell* **97,** 703–716 (1999).
14. Wichterle, H., Garcia-Verdugo, J. M. & Alvarez-Buylla, A. Direct evidence for homotypic, glia-independent neuronal migration. *Neuron* **18,** 779–791 (1997).
15. Marshall, C. A., Suzuki, S. O. & Goldman, J. E. Gliogenic and neurogenic progenitors of the subventricular zone: who are they, where did they come from, and where are they going? *Glia* **43,** 52–61 (2003).
16. Picard-Riera, N. *et al.* Experimental autoimmune encephalomyelitis mobilizes neural progenitors from the subventricular zone to undergo oligodendrogenesis in adult mice. *Proc. Natl Acad. Sci. USA* **99,** 13211–13216 (2002).
17. Menn, B. *et al.* Origin of oligodendrocytes in the subventricular zone of the adult brain. *J. Neurosci.* **26,** 7907–7918 (2006).
18. Spassky, N. *et al.* Adult ependymal cells are postmitotic and are derived from radial glial cells during embryogenesis. *J. Neurosci.* **25,** 10–18 (2005).

19. Lu, Q. R. *et al.* Common developmental requirement for Olig function indicates a motor neuron/oligodendrocyte connection. *Cell* **109,** 75–86 (2002).
20. Zhou, Q. & Anderson, D. J. The bHLH transcription factors OLIG2 and OLIG1 couple neuronal and glial subtype specification. *Cell* **109,** 61–73 (2002).
21. Scheffler, B. *et al.* Phenotypic and functional characterization of adult brain neuropoiesis. *Proc. Natl Acad. Sci. USA* **102,** 9353–9358 (2005).
22. Novak, A., Guo, C., Yang, W., Nagy, A. & Lobe, C. G. Z/EG, a double reporter mouse line that expresses enhanced green fluorescent protein upon Cre-mediated excision. *Genesis* **28,** 147–155 (2000).
23. Zappone, M. V. *et al.* Sox2 regulatory sequences direct expression of a β-geo transgene to telencephalic neural stem cells and precursors of the mouse embryo, revealing regionalization of gene expression in CNS stem cells. *Development* **127,** 2367–2382 (2000).
24. Parras, C. M. *et al. Mash1* specifies neurons and oligodendrocytes in the postnatal brain. *EMBO J.* **23,** 4495–4505 (2004).
25. Long, J. E. *et al.* Dlx-dependent and -independent regulation of olfactory bulb interneuron differentiation. *J. Neurosci.* **27,** 3230–3243 (2007).
26. Bernstein, B. E. *et al.* A bivalent chromatin structure marks key developmental genes in embryonic stem cells. *Cell* **125,** 315–326 (2006).
27. Milne, T. A. *et al.* MLL targets SET domain methyltransferase activity to *Hox* gene promoters. *Mol. Cell* **10,** 1107–1117 (2002).
28. Lee, M. G. *et al.* Demethylation of H3K27 regulates polycomb recruitment and H2A ubiquitination. *Science* **318,** 447–450 (2007).
29. Swigut, T. & Wysocka, J. H3K27 demethylases, at long last. *Cell* **131,** 29–32 (2007).
30. Mikkelsen, T. S. *et al.* Genome-wide maps of chromatin state in pluripotent and lineage-committed cells. *Nature* **448,** 553–560 (2007).

Supplementary Information is linked to the online version of the paper at www.nature.com/nature.

Acknowledgements We thank J. Rubenstein for anti-DLX2 antibodies and the pCAG-Dlx2 plasmid, D. Rowitch for anti-OLIG2 antibodies, and Y. Dou and R. Roeder for anti-MLL1 antibodies. This work was supported by the Neurosurgery Research and Education Foundation/American Association of Neurological Surgeons, Sandler Family Foundation, Northern California Institute for Research and Education, and the Clinical and Translational Research Institute at the University of California, San Francisco (D.A.L.), California Institute for Regenerative Medicine New Faculty Award and The Chicago Community Trust Searle Scholar Award (J.W.), and the Goldhirsch Foundation, J.G. Bowes Research Fund, and National Institutes of Health (NIH) 5R37-NS028478 (A.A.-B.).

Author Contributions D.A.L. conceived the project, designed and performed experiments, coordinated collaborations, and wrote the manuscript. Y.-C.H. worked on most experiments, quantified all *in vivo* data, and helped prepare the figures. T.S. and J.W. performed ChIP experiments, helped analyse data and contributed ideas. A.L.M and P.A.E. provided the *Mll1*$^{F/F}$ mouse, helped perform preliminary experiments in *Mll1*$^{+/-}$ mice and contributed ideas. J.M.G.V. provided electron microscopy data and histological interpretation. A.A.-B. contributed ideas, interpreted results and helped write the manuscript. All authors discussed the results and edited the manuscript.

Author Information Reprints and permissions information is available at www.nature.com/reprints. Correspondence and requests for materials should be addressed to D.A.L. (limd@neurosurg.ucsf.edu) or A.A-B. (abuylla@stemcell.ucsf.edu).

METHODS

Animals. *Mll1*$^{F/F}$ mice were maintained and genotyped as described[8]. *hGFAP-Cre*[9], *ZEG*[22] and *R26R* mice were obtained from Jackson Laboratories. To label proliferating cells, BrdU (10 mg ml^{-1} solution, 50 mg kg^{-1} body weight, Sigma) was injected intraperitoneally. Experiments were performed in accordance to protocols approved by Institutional Animal Care and Use Committee at UCSF.

Tissue preparation, immunohistochemistry and *in situ* hybridization. Brains were fixed by intracardiac perfusion as previously described[13]. Five-micrometre paraffin sections were used for H&E staining. For immunocytochemistry, 12-μm frozen sections were used with the following primary antibodies: mouse anti-GFAP (1:500, Chemicon), guinea pig anti-doublecortin (1:500, Chemicon), rat anti-BrdU (1:100, Abcam), anti-MASH (1:100 Pharmingen), rabbit anti-OLIG2 (1:10,000, gift from D. Rowitch), rabbit anti-DLX2 (1:1,000, gift from J. Rubenstein), rabbit anti-activated caspase 3 (1:500, Cell Signal Technology), anti-Nestin (1:500, Chemicon), rabbit anti-SOX2 (Abcam), mouse anti-S100 (1:500, Dako), mouse anti-MLL, N-terminal (1:500, Upstate), mouse anti-βIII-tubulin (Tuj1 clone, 1:250, Covance), mouse anti-myelin basic protein (1:2,000, Covance), mouse anti-O4 (1:50, Chemicon) and chicken anti-GFP (1:500, Aves). FluoroMyelin (Invitrogen) was used according to the manufacturer's protocols. Sections were blocked with 10% goat serum plus 0.3% Triton X-100 (Sigma) in PBS for 30 min at 25 °C, before primary antibody incubation at 4 °C overnight. BrdU staining was performed as in ref. 13. Goat Alexa-Fluor secondary antibodies (Invitrogen) were used, and nuclei were counterstained with DAPI (Sigma). *Mll1 in situ* hybridization was as previously described[5]. X-Gal staining and electron microscopy was performed as previously described[13].

Cell culture. Mouse SVZ monolayer cultures were produced essentially as previously described[21]. In brief, SVZ microdissections were dissociated with 0.25% trypsin and trituration. Cells were plated at ~30,000 cells cm^{-2} in 6-well plates (Corning) in proliferation medium (DMEM/F12/N2, 5% FCS, 20 ng ml^{-1} EGF, 20 ng ml^{-1} bFGF, 35 μg ml^{-1} bovine pituitary extract (media and N2 are from Invitrogen; growth factors are from Peprotech; FCS is from Hyclone). Non-attached cells were collected after 1 day and replated into 6-well plates. After ~7 days, the cells were confluent and these were routinely passaged 1:2 with 0.25% trypsin. Cells were passaged 4–6 times before use in experiments. Differentiation of cultures was induced by removing the EGF, FGF and FCS from the media[21]. For FACS, cells were dissociated with 0.25% trypsin and passed through a 40-μm mesh. A FACSAria (BD Biosciences) cell sorter with a 70-μm nozzle was used at the low pressure setting. Cells were collected into DMEM/F12 with 20% FCS. FACS isolated cells were centrifuged (500*g*, 15 min), resuspended in proliferation medium, and plated at ~100,000 cells cm^{-2}. For cell proliferation analysis, BrdU was used at 10 μM. For immunostaining, cultures were fixed with 4% paraformaldehyde. Primary and secondary antibodies were used as indicated above, with the exception that O4 staining was performed without Triton X-100. For plasmid transfections, SVZ cells were plated at ~75,000 cells cm^{-2} into 8- or 16-well Lab-Tek CCR2 chamber slides (Nunc) in proliferation medium. The next morning, 5 μg cm^{-2} of pCAG-GFP or both pCAG-GFP and pCAG-Dlx2 was transfected with Lipofectamine (Invitrogen). Twenty-four hours after transfection, differentiation was induced. Annexin A5 staining with APC-conjugated antibodies (BD Biosciences) was performed as per the manufacturer protocols and quantified on a fluorescent flow cytometer.

Microscopy and quantification. For quantification of cell cultures, at least five non-overlapping fields of view were analysed at the fluorescent microscope (Olympus AX70) with ×20 to ×60 objectives; in some cases, digital images were captured and immunostained cells were counted using Photoshop (Adobe Systems) or ImageJ (NIH) software. For *in vivo* SVZ cell quantification, we collected >3 non-overlapping confocal images from each tissue section using a Zeiss Axiovert 200M with a ×63-oil objective; from each animal, at least three separate tissue sections were analysed.

qRT–PCR. Total cellular RNA was isolated by Trizol method (Invitrogen) and quantified using the NanoDrop spectrophotometer. One microgram of total RNA was treated with Turbo DNase (Ambion) then reverse transcribed with VILO Superscript (Invitrogen). Complementary DNA corresponding to 5 ng of total RNA was used as a template in qPCR analysis performed on a Roche LC480 with SybrGreen (Roche). Relative expression for the studied genes was normalized to the mean signals of six mouse housekeeping genes: *Atpaf2*, *Dhps*, *Gapdh*, *Nosip*, *Pdha1* and *Tufm*.

Quantitative chromatin immunoprecipitation. qChIP was performed as essentially as previously described[31]. In brief, 10^7 cells were fixed for 10–20 min in 1% formaldehyde and then washed with 125 mM glycine. Cells were pelleted by centrifugation at 1,000*g*. After freeze-thawing, cells were suspended in 1 ml swelling buffer and separated by 20 strokes in a Dounce homogenizer. The cell suspension was pelleted and resuspended in 250 μl of lysis buffer, then sonicated in a Diagenode Bioruptor with ten 30 s pulses over a 15 min period at the high-energy setting. The cell lysate was pelleted by centrifugation at $1.6 \times 10^4 g$ for 15 min at 4 °C. The supernatant was diluted tenfold in ice-cold dilution buffer containing protease inhibitors (Roche) and subsequently cleared by centrifugation at $1.6 \times 10^4 g$ for 15 min at 4 °C. An aliquot of supernatant was reserved as the input control. The remaining portion was incubated overnight with the appropriate antibodies (H3K4 tri-methyl, Abcam; H3K27 tri-methyl, Upstate; MLL rabbit polyclonal, gift from D. Allis). Immune complexes were collected by 30 min incubation with Protein A Dynabeads, washed once with dilution buffer, five times with RIPA buffer and once with TE buffer. Complexes were eluted with 1% SDS and 0.84% $NaHCO_3$ solution. NaCl was added to 150 mM, and the eluates were decrosslinked by incubation at 65 °C overnight. The eluates were treated with RNase and proteinase K, extracted with phenol/chloroform and ethanol precipitated with glycogen as a carrier. An input control was processed in parallel. DNA was dissolved in ultrapure water and subjected to qPCR analysis with the Roche LC480 and SybrGreen. Serial dilutions of mouse genomic DNA was used for standardization. For qChIP and qRT–PCR, error estimates are standard deviations and were propagated by the least square formula. Recovery of genomic DNA as the percentage input was calculated as the ratio of copy numbers in the immunoprecipitate to the input control. Primer sequences are available on request.

31. Wysocka, J. *et al.* WDR5 associates with histone H3 methylated at K4 and is essential for H3 K4 methylation and vertebrate development. *Cell* **121**, 859–872 (2005).

SUPPLEMENTARY INFORMATION

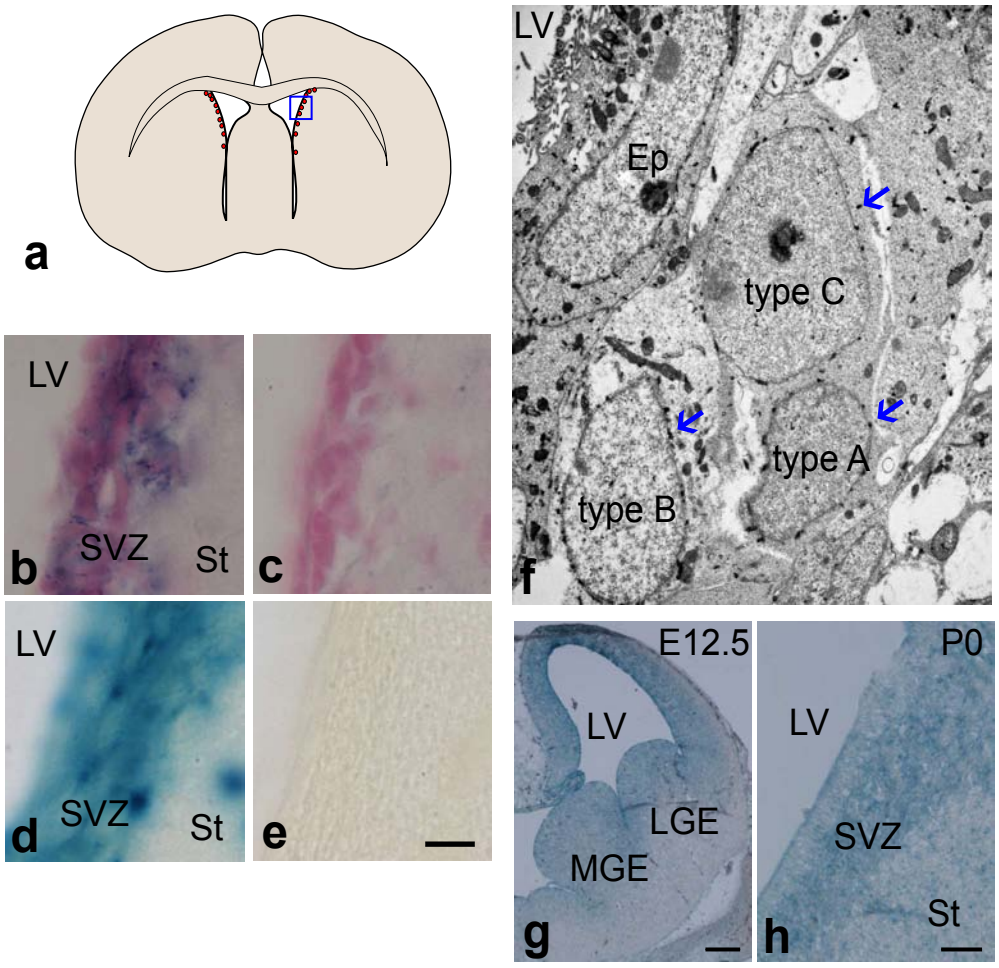

Supplementary Figure 1 | *Mll1* is expressed in postnatal and adult SVZ cells and in embryonic brain germinal zones. **a,** Coronal schematic indicating the germinal SVZ region (red dots). Blue box indicates regions in (b-e). **b-e,** *Mll1* expression was revealed by *in situ* hybridization (ISH) and *LacZ* expression in *Mll1* $^{LacZ/+}$ mice. Antisense probe to *Mll1* showed hybridization signal in SVZ cells (**b**, purple stain); the control sense probe (**c**) did not produce any signal; pink is a nuclear counterstain. **d-e**, X-gal histochemistry revealed LacZ expression in *Mll1* $^{LacZ/+}$ mice (**d**, blue X-gal deposit); control *Mll1* $^{+/+}$ mice did not have any LacZ activity (**e**). **f,** Electron microscopy of X-gal stained *Mll1* $^{LacZ/+}$ SVZ revealed X-gal deposit (indicated by blue arrows) in all SVZ cell types: type A = neuroblast, type B - SVZ stem cell, type C = transit-amplifying cell, Ep = ependymal cell. **g-h,** *Mll1* was also expressed in E12.5 cortical ventricular zone and ganglionic eminences (**g**) and P0 (**h**) SVZ (X-gal staining of *Mll1* $^{LacZ/+}$ mice). LV, lateral ventricle; St, striatum; LGE, lateral ganglionic eminence; MGE, medial ganglionic eminence; dapi, 4'6-diamidino-2-phenylindole. Scale bars, 10 μm (**b-e**), 100 μm (**g**), 50 μm (**h**).

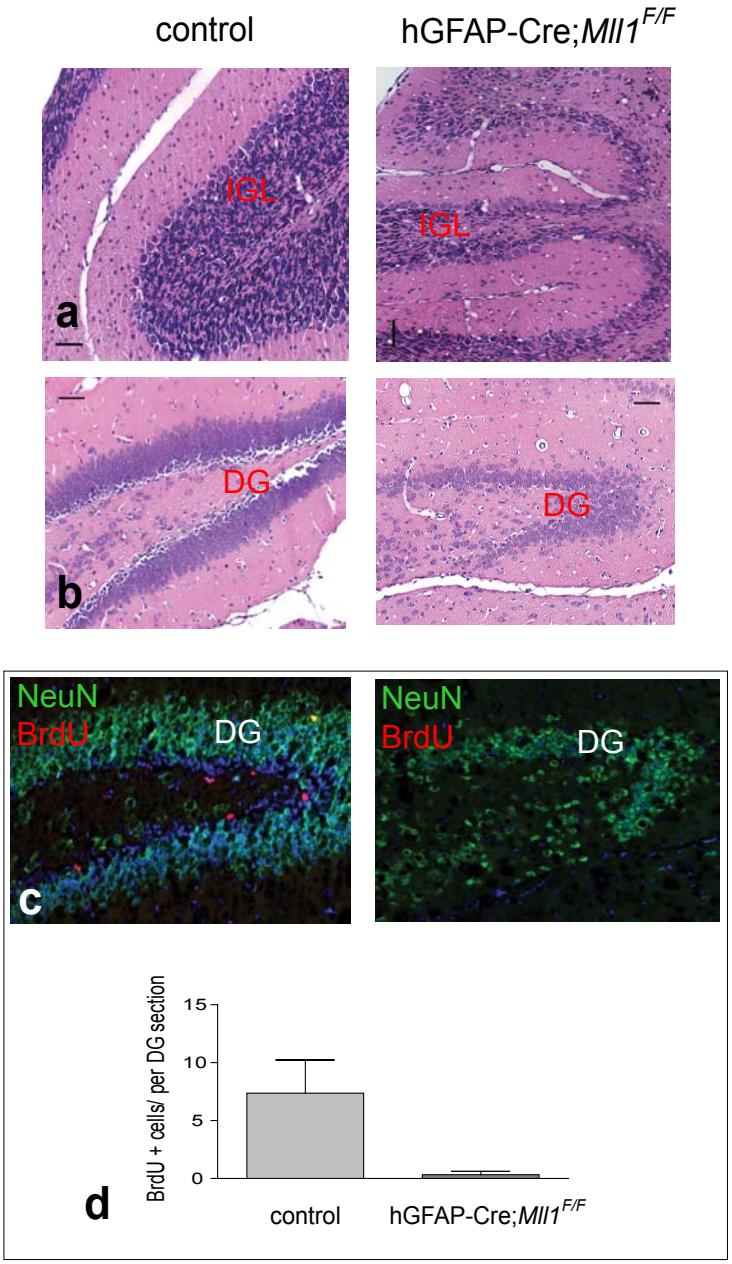

Supplementary Figure 2 | The cerebellar internal granular layer and hippocampal dentate gyrus show evidence of reduced neurogenesis in hGFAP-Cre;*Mll1* $^{F/F}$ mice. **a,** Hematoxylin-eosin stained sagittal sections through P25 cerebellum showed greatly reduced number of cells in the postnatally generated internal granular layer (IGL) of hGFAP-Cre;*Mll1* $^{F/F}$ mice (right panel) in comparison to controls (left panel). **b,** The dentate gyrus (DG) of hGFAP-Cre;*Mll1* $^{F/F}$ mice (right panel) is also hypocellular in comparison to controls (left panel). **c-d,** hGFAP-Cre;*Mll1* $^{F/F}$ mice have reduced DG cell proliferation at P25. Normally the DG remains neurogenic throughout postnatal and adult life. Mice were injected with the mitotic marker BrdU 1 h before sacrifice, and sections were stained for the neuronal marker NeuN (green) and Brdu (red). DG from hGFAP-Cre;*Mll1* $^{F/F}$ mice (**c,** right panel) have fewer NeuN+, BrdU+ cells in comparison to control (**c,** left). This difference in DG cell proliferation was quantified and is shown in d, (error bars indicate s.e.m., n=3 in each group). Scale bars, 20 μm.

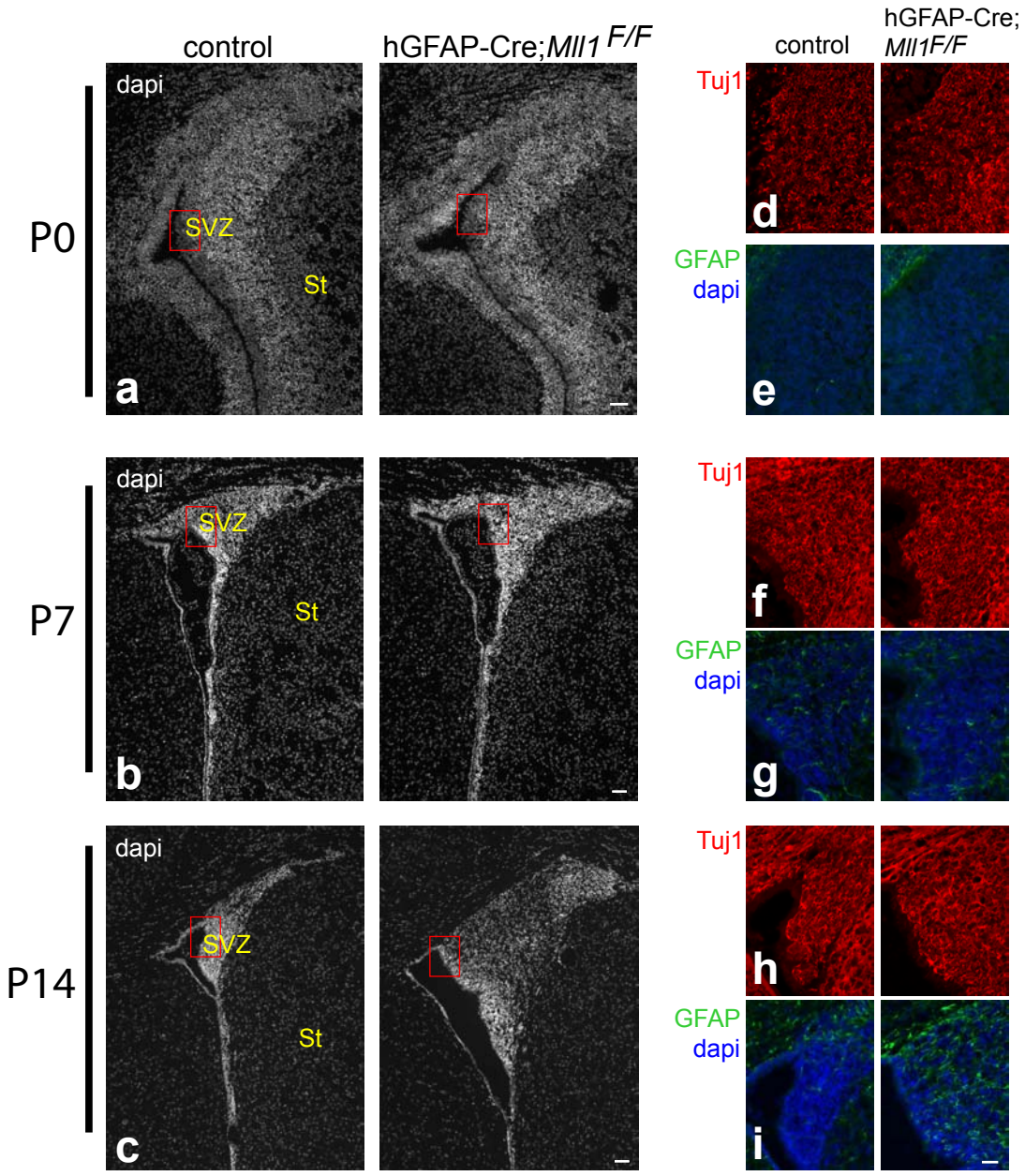

Supplementary Figure 3 | Neuroblasts accumulate in SVZ of hGFAP-Cre;*Mll1 F/F* mice postnatally. **a,d,e,** The SVZ of P0 mice is normally expanded as seen in dapi-stained sections (left panel), and the SVZ of hGFAP-Cre;*Mll1 F/F* mice is of a similar thickness (**a**, right panel). Red boxed areas in (**a**) are shown at higher magnification in the smaller panels to the right immunostained for Tuj1 (**d**) and GFAP (**e**). **b,f,g,** At P7, the SVZ is still of similar thickness (**b**), and Tuj1 (**f**) and GFAP expression (**g**) are also similar between control and hGFAP-Cre;*Mll1 F/F* mice. **c,h,i,** By P14, the SVZ of hGFAP-Cre;*Mll1 F/F* mice is significantly expanded (**c**, right), and GFAP expression is also increased (**i**, right). Scale bars, 100 μm (**a-c**), 20 μm (**i**).

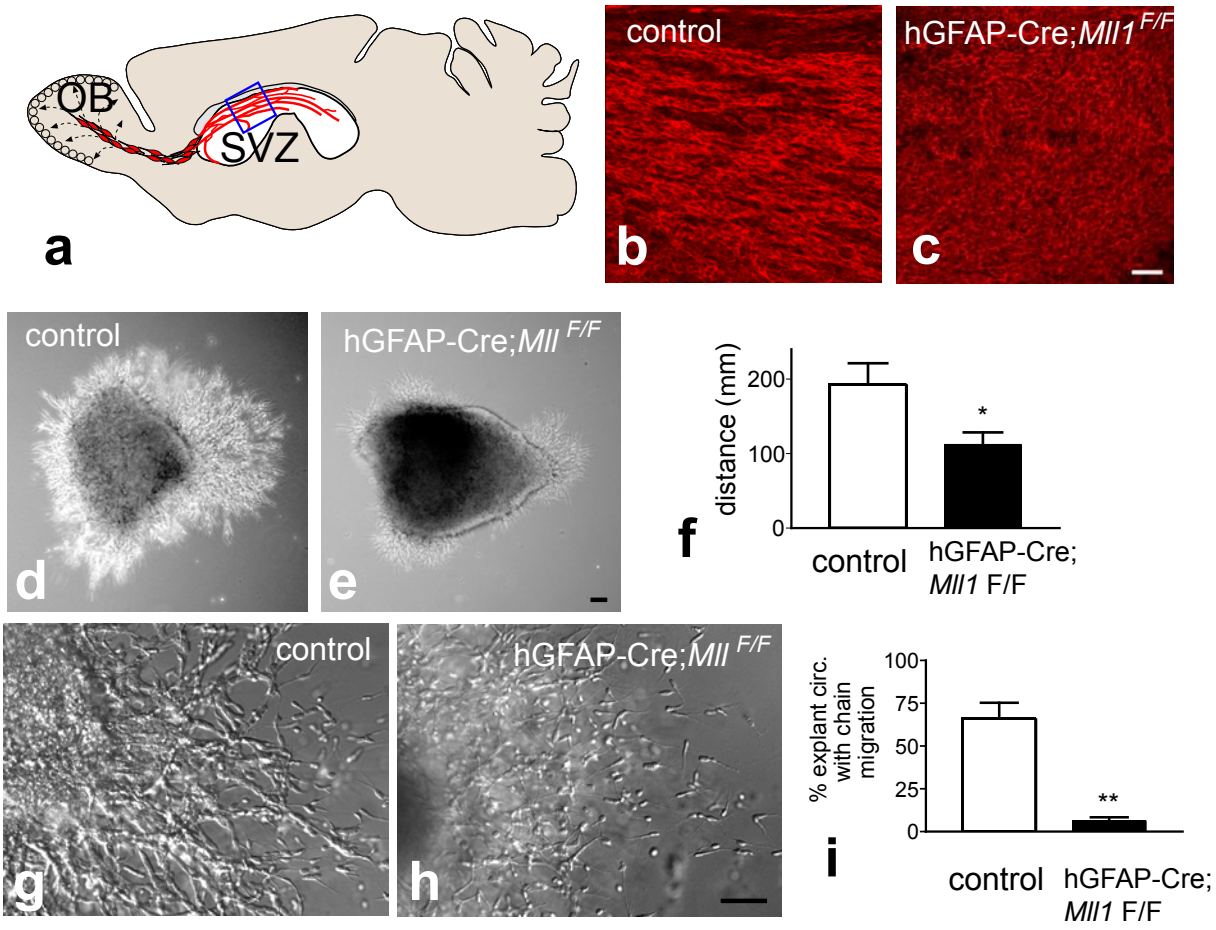

Supplementary Figure 4 | *Mll1* is required for normal SVZ neuroblast chain migration. **a,** Sagittal schematic showing normal paths of neuroblast migration from SVZ to OB. Blue box indicates regions shown in immunostained whole mount preparations shown in (**b-c**). **b-c,** Confocal images of DCX+ (red) neuroblasts in whole mount SVZ preparations. Image plane is parallel to the ventricle wall; anterior-posterior orientation is left-right. Control mice displayed DCX+ neuroblasts arranged in orderly chains (**b**), whereas in hGFAP-Cre;*Mll1* $^{F/F}$ mice, DCX+ cells were disorganized (**c**). **d-e,** Neuroblast migration from hGFAP-Cre;*Mll1* $^{F/F}$ SVZ explants (**e**) was decreased as compared to controls (**d**). **f,** Quantification of distance migrated in 18 h (error bars indicate s.e.m., n=21 control explants, n=35 hGFAP-Cre;*Mll1* $^{F/F}$ explants, **P*=0.01). **g-h,** Control explants (**g**) demonstrated normal chain migration of neuroblasts. In contrast, neuroblasts from hGFAP-Cre;*Mll1* $^{F/F}$ mice (**h**) migrate as single cells. **i,** The percentage of each explant circumference demonstrating chain migration was reduced by *Mll1*-deletion (error bars indicate s.e.m., n= 14 control explants, n=21 hGFAP-Cre;*Mll1* $^{F/F}$ explants, ***P*< 0.001). Scale bars, 50 μm.

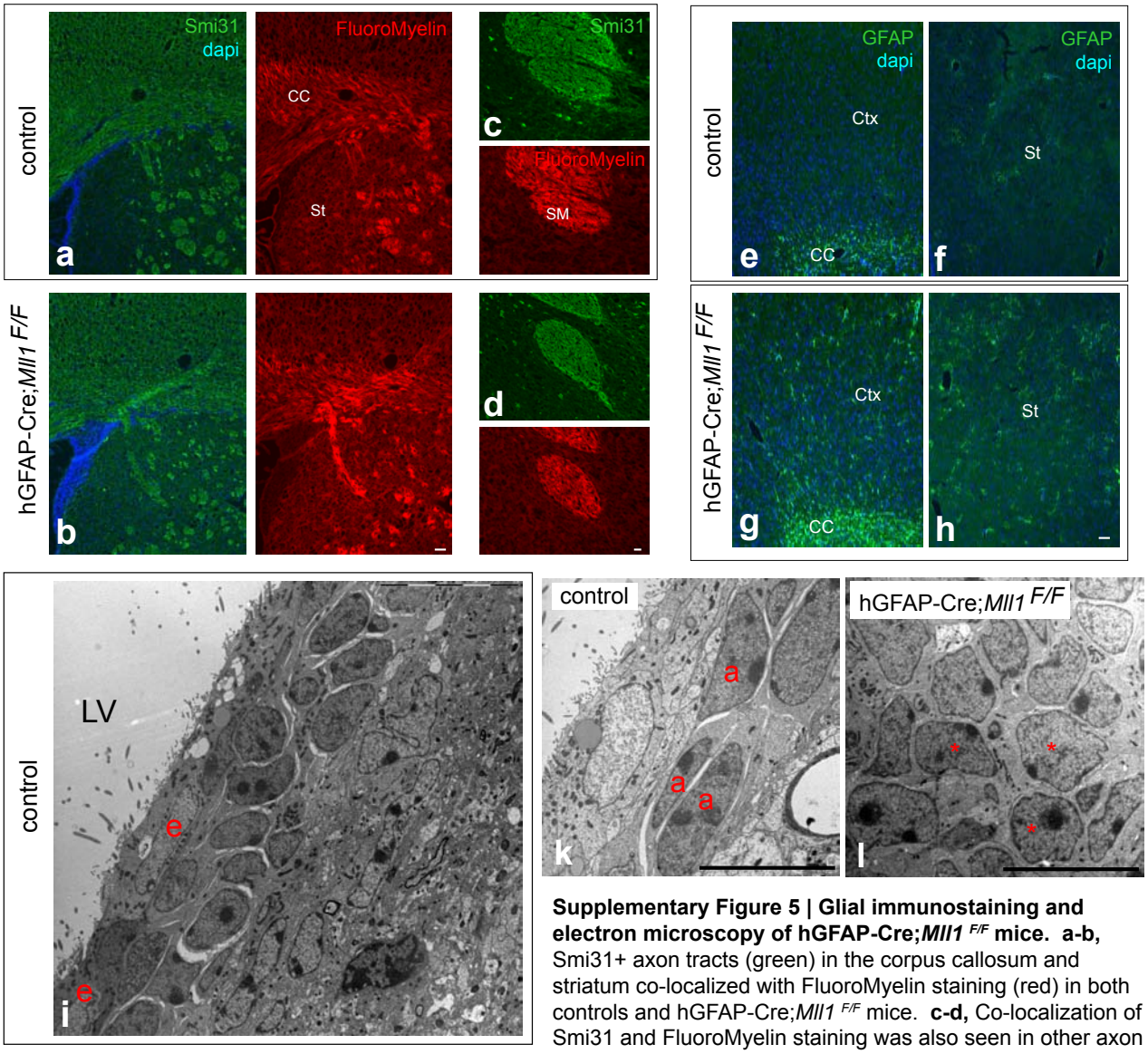

Supplementary Figure 5 | Glial immunostaining and electron microscopy of hGFAP-Cre;*Mll1* $^{F/F}$ mice. a-b, Smi31+ axon tracts (green) in the corpus callosum and striatum co-localized with FluoroMyelin staining (red) in both controls and hGFAP-Cre;*Mll1* $^{F/F}$ mice. **c-d,** Co-localization of Smi31 and FluoroMyelin staining was also seen in other axon bundles including the stria medullaris. **e-h,** GFAP+ astrocytes were more numerous in hGFAP-Cre;*Mll1* $^{F/F}$ mice in both the cortex (**g**) and striatum (**h**) as compared to controls (**e, f**). Images are from 12 μm frozen sections immunostained in parallel. **i-l,** EM analysis of SVZ. Ciliated ependymal cells (indicated by red "e") line the lateral ventricle (LV) wall in both control (**i**) and hGFAP-Cre;*Mll1* $^{F/F}$ mice (**j**). In normal mice, migratory neuroblasts (**k**, a cells) have elongated morphologies and smooth nuclear contours. In contrast, in hGFAP-Cre;*Mll1* $^{F/F}$ mice, many progenitors (* marks examples in **j**) are rounded as apposed to elongated, and the nuclei often have invaginations; these are characteristics of SVZ transit amplifying cells. However, these *Mll1*-deficient cells also have the ribosome content and lack of microtubules that are characteristic of neuroblasts. Thus, many SVZ cells in hGFAP-Cre;*Mll1* $^{F/F}$ mice have ultrastructural characteristics of both migratory neuroblasts and immature progenitors.
Scale bars, 50 μm (**b**), 20 μm (**d**), 100 μm (**h**), 10 μm (**i-l**). CC, corpus callosum; St, striatum; Ctx, cortex; SM, stria

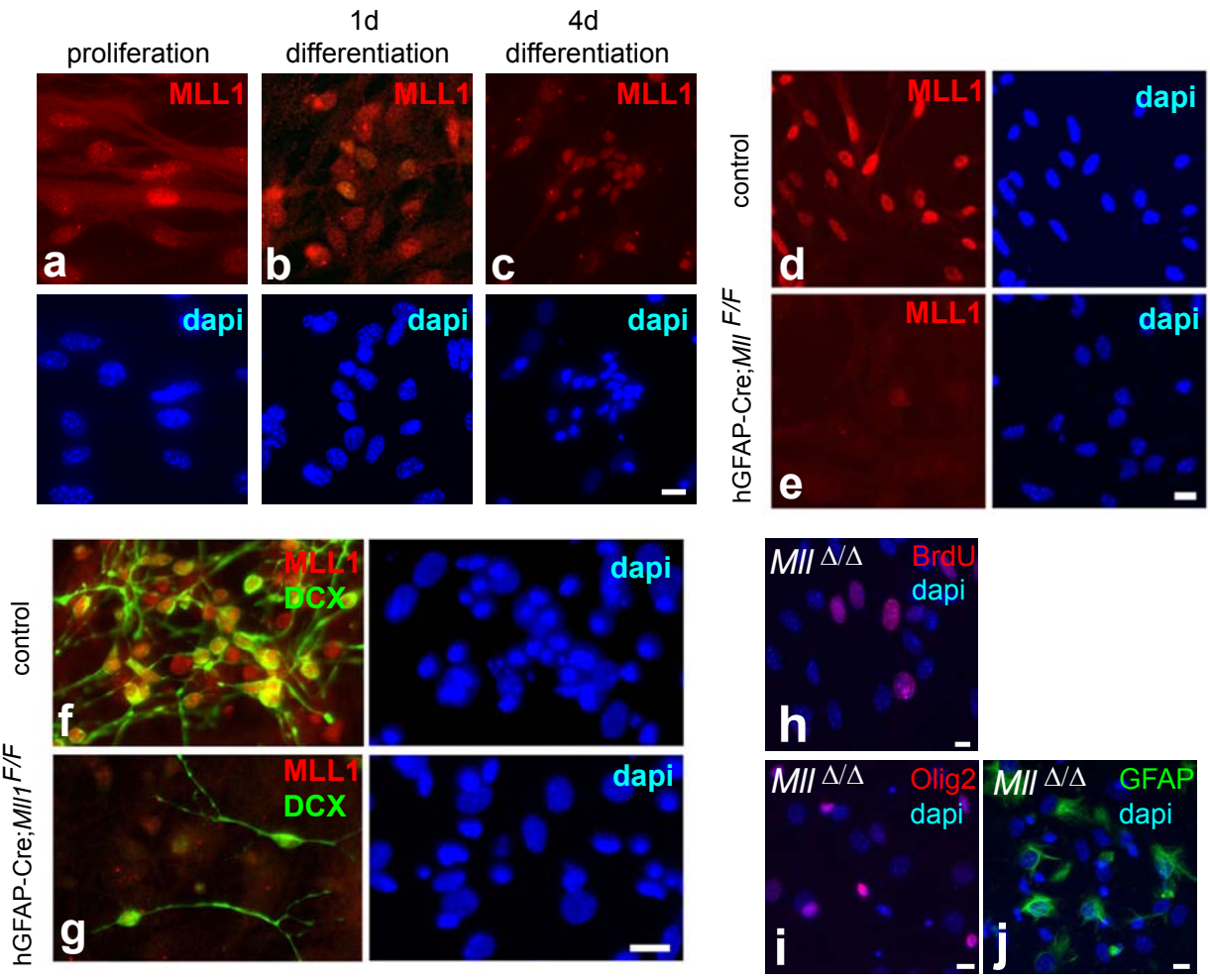

Supplementary Figure 6 | MLL1 immunocytochemistry and examples of *Mll1*-deleted glial cells. **a-c,** SVZ monolayer stem cell cultures express MLL1 under proliferating and differentiation conditions. MLL1 protein was detected by immunocytochemistry in control SVZ cultures under proliferation conditions (**a**) and after differentiation (**b**, 1 day), (**c**, 4 days). **d-e,** SVZ monolayer stem cell cultures from hGFAP-Cre;*Mll1* $^{F/F}$ mice do not express MLL1. SVZ cultures from control mice immunostained for MLL1 protein (**d,** red). In contrast, 95-96% of cells in SVZ cultures derived from hGFAP-Cre;*Mll1* $^{F/F}$ mice (**e**) did not express detectable MLL1 protein. **f,g** The few neuroblasts that develop from hGFAP-Cre;*Mll1* $^{F/F}$ cultures do not express MLL1 protein. DCX+ (green) neuroblasts in control cultures (**f**) expressed MLL1 protein (red), whereas the limited number of DCX+ neuroblasts in cultures from hGFAP-Cre;*Mll1* $^{F/F}$ mice did not have detectable MLL1 protein expression (**g**). **h-j,** *Mll1*-deleted SVZ cells proliferate (**h**, red BrdU+ cells) and differentiate efficiently into Olig2+ (**i**, red) and GFAP+ (**j**, green) cells. Quantification is in the main text (%BrdU+) and **Figure 2, f** (for glial differentiation). Scale bars, 20 μm.

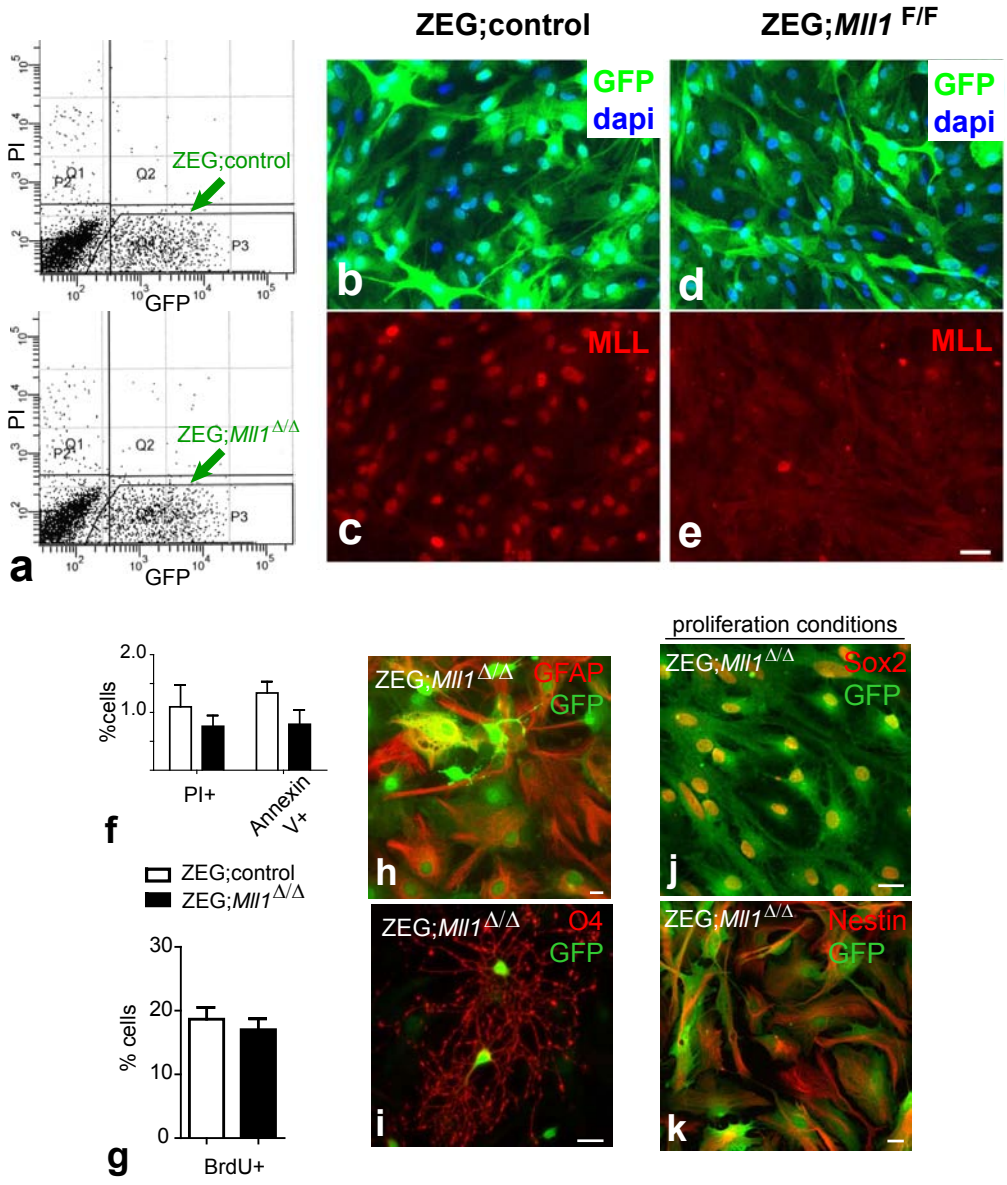

Supplementary Figure 7 | Analysis of FACS-isolated GFP+ cells from ZEG;*Mll1* $^{F/F}$ and control SVZ cultures. Cre-mediated recombination was induced in ZEG;*Mll1* $^{F/F}$ and ZEG;control monolayer cultures by infection with Cre-adenovirus. **a,** ZEG transgene cells become GFP+ after loxP site recombination, and these SVZ cells were isolated by FACS (x-axis, boxed areas). PI+ cells (y-axis) were excluded. **b-e,** GFP+ cells from ZEG;*Mll1* $^{F/F}$ cultures do not express MLL protein. GFP+ cells from ZEG;control cultures (**b**) all had detectable MLL1 protein (**c**). GFP+ cells from ZEG;*Mll1* $^{F/F}$ cultures (**d**) were > 97% negative for MLL1 immunocytochemistry (**e**). **f,** Cell death in proliferating SVZ cells was not increased by *Mll1*-deletion as indicated by flow-cytometric analysis of PI+ or Annexin V+ cells. **g,** BrdU incorporation rate was unchanged by *Mll1*-deletion (quantification of immunostained cultures). **h-i,** ZEG;*Mll1* $^{\Delta/\Delta}$ cells efficiently produced GFAP+ astrocytes (**h**) and O4+ oligodendrocytes (**i**). Quantification is in **Figure 3**, main text. j-k, Proliferating ZEG;*Mll1* $^{\Delta/\Delta}$ cells expressed neural stem cell markers Sox2 (**k**) and and Nestin (**k**). Scale bars, 50 μm (**e**), 20 μm (**h-k**).

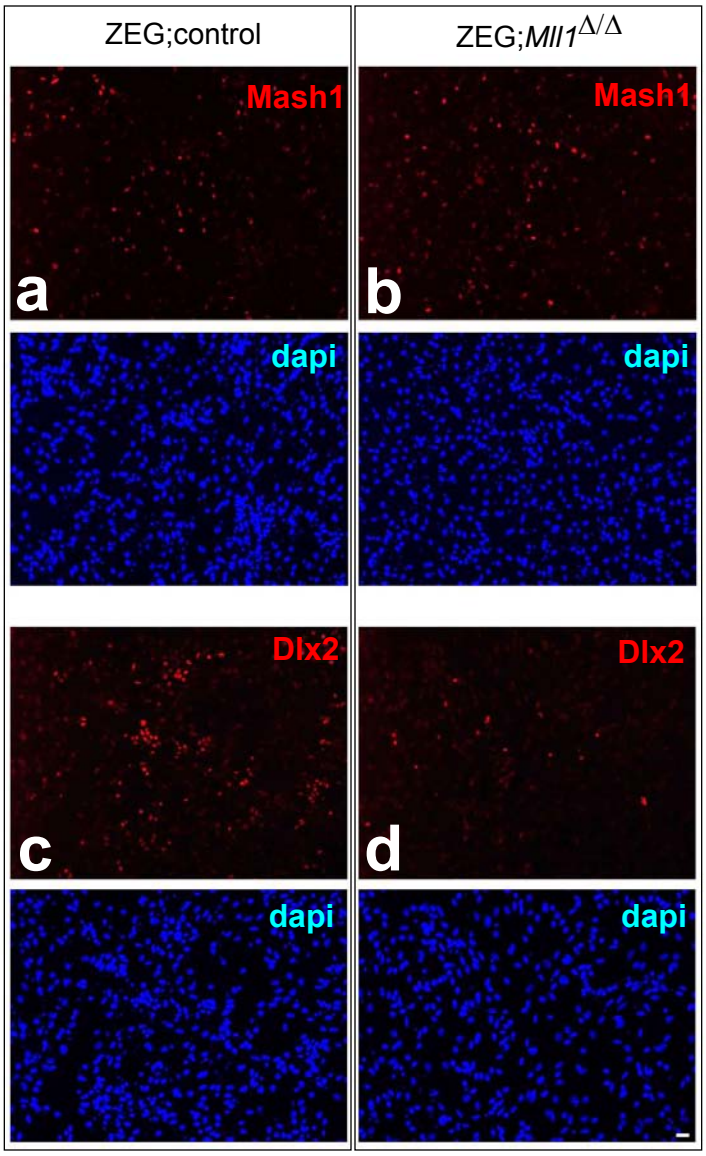

Supplementary Figure 8 | *Mash1* expression is maintained in ZEG;*Mll1* $^{\Delta/\Delta}$ SVZ cells during differentiation, but *Dlx2* expression is not. ZEG;control cultures (**a**) and ZEG;*Mll1* $^{\Delta/\Delta}$ cultures (**b**) had similar levels of *Mash1* expression at differentiaton day 2. At this same time point, *Dlx2* expression was decreased in ZEG;*Mll1* $^{\Delta/\Delta}$ cultures (compare panels **c** and **d**). Quantification of repeat experiment is in **Figure 3f**. Scale bar, 50 μm.

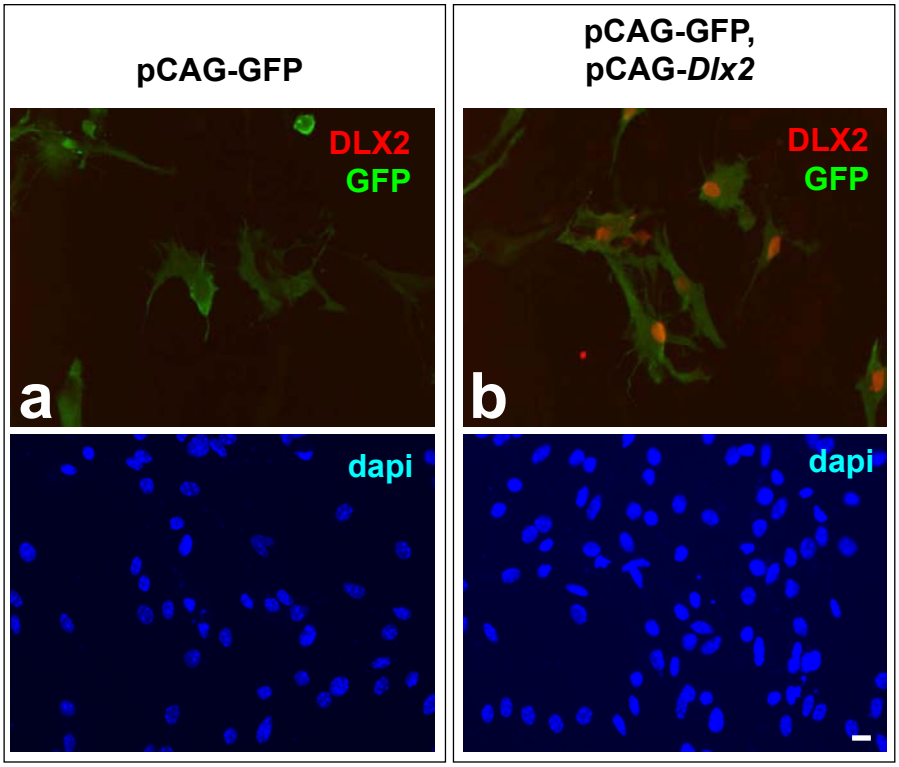

Supplementary Figure 9 | Co-transfection of pCAG-*Dlx2* and pCAG-GFP plasmids results in GFP and DLX protein co-expression in *Mll1*-deleted SVZ monolayer cultures. **a,** There were no DLX2+ cells in control pCAG-GFP transfected cultures. **b,** ~85% of GFP+ cells were immunopositive for DLX2 (red) when pCAG-GFP and pCAG-*Dlx2* plasmids were co-transfected. Scale bars, 20 μm.